




Functional Dynamics of Neutrophils After Ischemic Stroke

Wei Cai^{1,2} · Sanxin Liu¹ · Mengyan Hu¹ · Feng Huang² · Qiang Zhu¹ · Wei Qiu¹ · Xiaoming Hu³ · Jacob Colello⁴ · Song Guo Zheng⁴  · Zhengqi Lu¹

Received: 29 September 2018 / Revised: 11 February 2019 / Accepted: 13 February 2019 / Published online: 7 March 2019
© Springer Science+Business Media, LLC, part of Springer Nature 2019

Abstract

Neutrophils are forerunners to brain lesions after ischemic stroke and exert elaborate functions. However, temporal alterations of cell count, polarity, extracellular trap formation, and clearance of neutrophils remain poorly understood. The current study was aimed at providing basic information of neutrophil function throughout a time course following stroke onset in patients and animal subjects. We found that neutrophil constitution in peripheral blood increased soon after stroke onset of patients, and higher neutrophil count indicated detrimental stroke outcomes. Comparably, neutrophil count in peripheral blood of stroke mice peaked at 12 h after cerebral ischemia, followed by a 1-2-day spike in brain lesions. In stroke lesion, clearance of neutrophils peaked at 2 days after stroke and extracellular traps were mostly detected at 2–3 days after stroke. In neutrophil infiltrated into stroke lesion, expression of the N2 marker CD206 was relatively stable. We found that the N2 phenotype facilitated neutrophil clearance by macrophage and did not further induce neuronal death after ischemic injury compared with N0 or N1 neutrophils. Skewing neutrophil toward the N2 phenotype before stroke reduced infarct volumes at 1 day after tMCAO. Conditioned medium of ischemic neurons drove neutrophils away from the protective N2 phenotype and increased the formation of extracellular traps. Conclusively, neutrophil function has an important impact on stroke outcomes. Neutrophil frequency in the peripheral blood could be an early indicator of stroke outcomes. N2 neutrophils facilitate macrophage phagocytosis and are less harmful to ischemic neurons. Directing neutrophils toward the N2 phenotype could be a promising therapeutic approach for ischemic stroke.

Keywords Brain ischemia · Neutrophils · Extracellular traps · Neuroprotection

Introduction

Cerebral ischemic stroke is a multiphasic disorder [1, 2]. Following the primary ischemic injury, inflammatory responses cause secondary exacerbation to the lesion. Neutrophils are among the forerunners to the ischemic brain after cerebral ischemia [3, 4]. Once summoned by neutrophil

attracting chemokines [5] to the stroke lesion, neutrophils display functional heterogeneity. Polarization of neutrophils toward the N2 phenotype has been demonstrated to be protective in ischemic stroke [6]. After executing their function, neutrophils are cleared by microglia/macrophages, which is facilitated by N2 polarization [6]. Neutrophil extracellular traps (NETs) were considered a programmed cell death

Wei Cai, Sanxin Liu and Mengyan Hu contributed equally to this work.

Electronic supplementary material The online version of this article (<https://doi.org/10.1007/s12975-019-00694-y>) contains supplementary material, which is available to authorized users.

✉ Song Guo Zheng
SongGuo.Zheng@osumc.edu

✉ Zhengqi Lu
lzq1828@outlook.com

¹ Department of Neurology, the Third Affiliated Hospital of Sun Yat-sen University, 600 Tianhe Road, Guangzhou, Guangdong 510630, People's Republic of China

² Center of Clinical Immunology, the Third Affiliated Hospital of Sun Yat-sen University, Guangzhou, People's Republic of China

³ Pittsburgh Institute of Brain Disorders and Recovery, and Department of Neurology, University of Pittsburgh School of Medicine, Pittsburgh, PA 15213, USA

⁴ Department of Internal Medicine, Ohio State University College of Medicine and Wexner Medical Center, Columbus, OH 43201, USA

mechanism to combat invading microorganisms [7]. It is not until recently that NETs were detected in aseptic inflammatory lesions [8]. To date, no evidence of NET formation in ischemic brain or its influence to injured neurons has been documented.

Neutrophils exert elaborate functions in the ischemic brain. Nevertheless, the time course of the aforementioned processes has not been fully explored. The aim of the current study was to depict the functional dynamics of neutrophils after ischemic stroke, including the time course of neutrophil infiltration, polarization, and clearance by microglia/macrophages. NET formation after ischemic stroke was analyzed. Interaction between ischemic neuron and neutrophil was also explored.

Materials and Method

Patients

The current research was approved by the ethics committee of the Third Affiliated Hospital of Sun Yat-sen University. Clinic files of 294 consecutive Chinese patients (ethnic Han) with acute ischemic stroke (AIS) admitted within 24 h of symptom onset in the Third Affiliated Hospital from January 1st, 2014, to August 10th, 2018 were reviewed. Among them, 17 patients were diagnosed as secondary ischemic stroke, 11 patients with malignant tumor, and 9 patients with cerebral hemorrhagic transformation. Additionally, 32 patients who had no magnetic resonance imaging (MRI) data were excluded. Altogether, 225 patients were included in the study, 58 of which had infection (including respiratory infection and urinary infection) and 167 without. Among those with infection, 34 patients had infarction > 1.5 cm and 24 had infarction ≤ 1.5 cm [9–11]. In patients without infection, 74 of them had infarction > 1.5 cm and 93 of them had infarction ≤ 1.5 cm. The inclusion process is shown in Fig. S1. Age (mean 64.87 ± 0.60 and 95% CI 63.69–66.05), gender (female:male = 68:157), and score of the National Institute Stroke Scale [12, 13] (NIHSS) of patients were recorded. Neutrophil count, neutrophil to lymphocyte ratio (NLR) in the peripheral blood, and the infarct sizes within 24 h after symptom onset were analyzed. A total of 56 age- and gender-matched healthy controls (HC) were included in the study. Patient demographics including comorbidities are summarized in Table S1.

Animals

C57BL/6 wild-type mice (8 to 12 weeks old, weight 18–25 g) were purchased from Guangdong Medical Laboratory Animal Center (Guangzhou, China) and housed in a humidity- and temperature-controlled animal facility in Sun Yat-sen University with a 12-h light–dark cycle for at least 1 week before induction of ischemic stroke. Food and water were

freely accessible. All the experimental protocols were approved by the Animal Care and Use Committee of Sun Yat-sen University following the Guide for the Care and Use of Laboratory Animals. A total of 152 male mice were used in the transient middle cerebral artery occlusion (tMCAO) model, including 20 mice that were excluded from further assessments due to death after ischemia or unsuccessful induction of stroke. The mortality rate was 0% in 1- and 3-h stroke mice, 10% in 6-h stroke mice, 18.18% in 12-h stroke mice, 25% in 1-day stroke mice, 25% in 2-day stroke mice, 25% in 3-day stroke mice, 33.33% in 5-day stroke mice, 42.86% in 7-day stroke mice, and 0% in sham animals. There were 30 male mice used for primary neutrophil- or macrophage-enriched culture, and 6 pregnant mice used for primary cortical neuronal culture.

Experiment Protocol

Experiment 1

Neutrophil alteration in patients with acute ischemic stroke and its correlation with stroke outcomes were evaluated. Neutrophil counts and NLR in the peripheral blood of patients and HC were assessed. NIHSS scores and infarct sizes of patient on admission were analyzed. Correlation analysis of NIHSS scores/infarct sizes with neutrophil counts/NLR was conducted.

Experiment 2

Numbers of neutrophil in infarct brain and peripheral blood could be influenced with infection, and infection commonly occurs after stroke due to immune compromise. As to better exclude the impact of infection on neutrophil fluctuation and testify the correlation between neutrophil elevation and infarct sizes, mice were pretreated with broad spectrum antibiotics to prevent infection. Cerebral ischemia was then induced and correlation analysis between neutrophil frequency in blood and infarct volumes of mice was performed. Internal comparison of the cohort was conducted with all animals pretreated with antibiotics.

Experiment 3

So as to investigate temporal, spatial, and functional dynamics of neutrophils after stroke, cerebral ischemia was induced in mice and samples were collected at various time points. Neutrophil percentages in bone marrow, peripheral blood and spleen, infiltration pattern in ischemic brain lesion, phenotypic shift, extracellular trap formation, and withdrawal time line were assessed with flow cytometry at 6 and 12 h and 1, 2, 3, 5, and 7 days after stroke. Expression of neutrophil

attracting chemokines and neutrophil functional factors in ipsilateral brain was evaluated with real-time polymerase chain reaction (RT-PCR) at 1, 3, 6, 12, 24, and 48 h after cerebral ischemia. To visualize NETs in stroke lesion, immunostaining of citrullinated histone H3 (CitH3) or Sytox Green and neutrophil elastase (NE) in brain slices and scanning electronic microscopy (SEM) experiments were performed.

Experiment 4

In order to evaluate the impact of neutrophil polarity and NET formation on phagocytosis in macrophages, N0, N1, N2, and NET-forming neutrophils were prepared and subjected to macrophages for phagocytosis. The numbers of neutrophils engulfed by macrophages were calculated.

Experiment 5

So as to investigate the impact of neutrophil polarity to stroke outcomes, neutrophil was skewed to N2 phenotype with transforming growth factor beta (TGF β). Comparison of infarct volumes between the TGF β -treated mice with PBS-treated controls was conducted.

Experiment 6

To evaluate the interaction between neutrophils and ischemic neurons, *in vitro* experiments were performed. Primary cultured mice neurons were subjected to oxygen glucose deprivation (OGD), followed by co-culturing with various phenotypes of neutrophils or treatment with neutrophil conditioned medium (CM). Viability of the ischemic neurons after a 24-h treatment was assessed with immunostaining of neuronal nuclei (NeuN). Furthermore, conditioned medium of post-OGD neurons was collected and treated with N0 neutrophils. Neutrophil polarization and NET formation after treatment were analyzed.

MRI Scanning and Infarct Volume Analysis of Patients

MRI was performed within 24 h of admission using 1.5- or 3.0-T magnetic resonance imaging (Signa; GE Medical Systems, Milwaukee, WI, USA). In this study, the diffusion-weighted imaging (DWI) spin-echo planar sequence included 20 contiguous axial oblique slices ($b = 0$ and 1000 s/mm^2 isotropically weighted; repetition time/echo time, 6000/60.4 ms; acquisition matrix, 128×128 ; slice thickness, 5 mm; interslice gap, 1 mm; field of view, 24 cm). DWI lesions in 225 patients were measured with Analyze 7.0 software (Analyze Direct, KS). Cerebral infarct sizes were assessed by largest infarct diameter determined on the image demonstrating the largest lesion [14]. MRI scans of patients were assessed by experienced neurologists Zhengqi Lu and

Sanxin Liu, who were blinded to the patients' clinical features. All images were interpreted with the same window settings and the same types of monitors and lighting conditions.

Murine Model of Transient Focal Ischemia

The focal ischemic stroke model was induced in mice with tMCAO as described previously [15]. Briefly, mice were anesthetized with 1.5% isoflurane in air under spontaneous breathing. A midline neck incision was made and soft tissues over the trachea were retracted gently. The left common carotid artery (CCA) was isolated and ligated temporarily. A permanent knot was placed on the distal part of external carotid artery (ECA) and a loose temporal knot was placed on both the proximal part of ECA. A tight temporal knot was placed on the internal carotid artery (ICA). ECA was cut between the permanent knot and the temporal knot, a filament was inserted into ECA and directed to middle cerebral artery (MCA) through ICA after loosening the temporal knot on ICA. Once the filament insertion into the MCA was confirmed, the loose temporal knot on ECA was tightened and the temporal knot on CCA was loosened. Filament insertion into the ICA was maintained for 60 min followed by reperfusion. Sham-operated animals underwent the same anesthesia and surgical procedures but were not subjected to arterial occlusion. Core body temperatures were maintained with a heating pad. Regional cerebral blood flow (rCBF) during the surgery was measured by laser Doppler flowmetry. Mice with less than 70% reduction of blood flow in the ischemic core or those which died during surgery were excluded from further analysis. To skew neutrophil polarization toward N2 phenotype, TGF β (2 μg per mouse) was *i.v.* injected to animals at 1 day before tMCAO. Blood samples were collected at 1 day after TGF β injection right before tMCAO surgery and neutrophil polarity was assessed.

Immunofluorescence Staining and Quantification

Mice were sacrificed at 6 and 12 h and 1, 2, 3, and 5 days after tMCAO and perfused with saline followed by PBS containing 4% paraformaldehyde (PFA, Sigma-Aldrich). Brains were removed and cut into 25- μm frozen cryosections using a microtome. Brain sections were incubated with primary antibodies at 4 °C overnight. After washing in PBS, sections were incubated with secondary antibodies for 1 h at room temperature. Sections were then washed and mounted with DAPI Fluoromount-G (Southern Biotech). The following primary antibodies were used: rat anti-Ly6G (1:500, BD Biosciences), goat anti-Iba1 (1:500, Abcam), goat anti-CD206 (1:500, R&D Systems), rabbit anti-CitH3 (1:500, Abcam), and rabbit anti-MPO (1:500, R&D Systems). The following secondary antibodies were applied: anti-rabbit secondary antibody conjugated with Cy3 (1:1000, Jackson

ImmunoResearch Laboratories), anti-rabbit secondary antibody conjugated with Alexa Fluor 488 (1:1000, Jackson ImmunoResearch Laboratories), anti-rat secondary antibody conjugated with Alexa Fluor 488 (1:1000, Jackson ImmunoResearch Laboratories), and anti-goat secondary antibody conjugated with Alexa Fluor 488 (1:1000, Jackson ImmunoResearch Laboratories). For detection of formation of NETs, brain sections from mice sacrificed at 2 days after tMCAO were stained with chromatin dye Sytox Green (Invitrogen, 5 mM in Hanks' balanced salt solution (HBSS)) and NE (1:200 Abcam). To assess neuronal viability, neurons were cultured on coverslips. After fixation with PBS containing 4% paraformaldehyde (Sigma-Aldrich), coverslips were incubated with rabbit anti-NeuN (1:500, Abcam) overnight. Coverslips were then washed and incubated with anti-rabbit secondary antibody conjugated with Cy3 (1:1000, Jackson ImmunoResearch Laboratories). Quantification of cell count was performed with ImageJ software by an investigator who was blinded to the experimental design (National Institutes of Health). The stroke core was identified as the region in which the majority of DAPI-stained nuclei were shrunken. The stroke penumbra was defined as the region of generally morphologically normal cells, approximately 450–500 μm from the boundary of the ischemic core.

Flow Cytometric Analysis

Single cells from brain, bone marrow, blood, and spleen were prepared for flow cytometric analysis (FACS) at 6 and 12 h and 1, 2, 3, 5, and 7 days after tMCAO. Bone marrow, blood, and spleen were extracted before animals were perfused with ice-cold saline. Brains were dissected, and ipsilateral hemispheres were collected after saline perfusion. Each hemisphere was subjected to 0.25% trypsin–EDTA (Thermo Fisher) digestion at 37 °C for 25 min. Brain tissue was then pressed through a cell strainer (70 μm , Thermo Fisher). Brain cells were separated from myelin debris by centrifugation in 30%/70% Percoll solution (GE Healthcare). Brain cells at the interface were collected, washed with PBS, and subjected to further staining. The spleen was homogenized and pressed through a cell strainer (40 μm , Thermo Fisher). Red blood cell lysis buffer (Sigma-Aldrich) was applied to get rid of red blood cells in the bone marrow, spleen, and blood. Bone marrow cells, spleen cells, and blood leukocytes were then subjected to further staining.

Single cells from the brain, spleen, and blood were stained with CD45-PerCp/Cy5.5 (1:400, BioLegend), CD11b-PE (1:400, BioLegend), Ly6G-APC/Cy7 (1:400, BioLegend), F4/80-BV421 (1:400, BioLegend), CD206-Alexa Fluor 647 (1:200, BD Biosciences), and MPO-FITC (1:400, Abcam). In the NLR analysis of peripheral blood, leukocytes were stained with CD45-PerCp/Cy5.5 (1:400, BioLegend), Ly6G-APC/Cy7 (1:400, BioLegend), F4/80-BV421 (1:400,

BioLegend), CD3-PE (1:400, BioLegend), and B220-PE (1:400, BioLegend). In the phenotypic analysis of primary culture neutrophil, cells were fixed, permeabilized, and then stained with CD206-Alexa Fluor 647 (1:200, BD Biosciences) and IL10-PE (1:100, BioLegend). Flow cytometric analysis was performed using a fluorescence-activated cell sorter flow cytometer (BD Biosciences), and data was analyzed using FlowJo X 10.0.7r2 software. In experiments analyzing the engulfed and unengulfed neutrophil by macrophages in stroke lesion, brain cells from the ipsilateral hemisphere were stained with antibody cocktail such as anti-CD45-PerCp/Cy5.5, anti-CD11b-PE, anti-Ly6G-APC/Cy7, and anti-F4/80-BV421. Ly6G is a specific marker for neutrophil, while F4/80 is a specific marker for macrophage. Before permeabilization, myeloid cells could rarely be co-stained with Ly6G and F4/80. After permeabilization, neutrophil engulfed by F4/80⁺ macrophage could be positively stained with Ly6G. Therefore, neutrophil was first gated with CD45^{hi}CD11b⁺Ly6G⁺, then those engulfed by macrophages were determined as F4/80⁺ (CD45^{hi}CD11b⁺Ly6G⁺F4/80⁺) cells, while those unengulfed were F4/80⁻ (CD45^{hi}CD11b⁺Ly6G⁺F4/80⁻).

Magnetic Sorting of Neutrophils

Single brain cells were prepared as previously mentioned. Four ischemic hemispheres were pooled and stained using Biotin-anti-Ly6G (BioLegend) with 1 μg antibodies per 10⁶ cells. Cells were washed with PBS and further stained with anti-Biotin microbeads (Miltenyi Biotec) for 1 μg antibodies per 10⁶ cells. After two washes with PBS, cells were subjected to positive selection program using autoMACS (Miltenyi Biotec). Cells were washed and then stained with goat anti-CD206 (1:500, R&D Systems) or rabbit anti-MPO (1:500, R&D Systems) for 30 min at room temperature. After three washes, cells were dropped on slides and mounted with Fluoromount-G (Southern Biotech).

Real-Time Polymerase Chain Reaction

Total RNA was isolated from the brains and primary cultured neutrophils using the RNeasy Mini Kit (QIAGEN) according to the manufacturer's instructions. The integrity of total RNA was evaluated using a denaturing agarose gel stained with ethidium bromide. One microgram RNA ($\text{OD}_{260\text{ nm}}/\text{OD}_{280\text{ nm}} = 1.8\text{--}2.2$) was used to synthesize the first strand of cDNA using the Prime Script RT reagent Kit (Takara). PCR was performed on a 7500 fast (ABI) RT-PCR machine using SYBR Premix Ex Taq (Takara). The following primers were used (mouse): CCL5 F: AAGTGTGTGCCAAC CCAGAG, CCL5 R: CCCATTTTCCCAGGACCGAG; CXCL1 F: TGGCTGGGATTACACTCAAG, CXCL1 R: CCGTTACTTGGGGACACCTT; CXCL2 F: CATAGCCA

CTCTCAAGGGCG, CXCL2 R: AGGTACGATCCAGG CTTCCC; CXCL3 F: CATCCAGAGCTTGACGGTGA, CXCL3 R: ACACATCCAGACACCGTTGG; CXCL5 F: CCCCTTCTCAGTCATAGCC, CXCL5 R: CTTCCACC GTAGGGCACTG; CXCL7 F: CCTGGCGTCAAGAG AATCGT, CXCL7 R: CTTGGCTTGCCCGTCTTCAT; MMP1a F: ACTACAACGACAACCCAAGAAA, MMP1a R: AGCTGGGCACAATAGGGATT; MMP2 F: AACGGTCGGGAATACAGCAG, MMP2 R: GTAAACAA GGCTTCATGGGGG; MMP3 F: CCCTGGGACTCTAC CACTCA, MMP3 R: AGTCTGAGAGATTTGCGCC; MMP8 F: CCACACACAGCTTGCCAATG, MMP8 R: GCTTCTTGCAACCATCGTG; MMP9 F: CCAGCCGA CTTTTGTGGTCT, MMP9 R: TGGCCTTTAGTGTC TGGCTG; MMP10 F: ATGGAACTTGACCCCTCAG, MMP10 R: GGTGGAAGTTAGCTGGGCTT; MMP13 F: GGAGCCCTGATGTTTCCCAT, MMP13 R: ATCAAGGG ATAGGGCTGGGT; TIMP1 F: GAGACACACCAGAG CAGATACC, TIMP1 R: TGGTCTCGTTGATTTCTGGG G; TIMP2 F: CAGCCTCTCCCGTCTTTTGT, TIMP2 R: GTGGCTAGAAACCCAGCAT; IFN α F: CTGGTCAA CCTGCTCTCTAGG, IFN α R: ACTTAGGACAGGGA TGGCTTTCT; IFN γ F: ATGAACGCTACACACTGCATC, IFN γ R: CCATCCTTTTGCCAGTTCCTC; IL-12a F: CCTTGCATCTGGCGTCTACA, IL-12a R: GTCTTACG CAGGTTTCGGGA; IL-23 F: TGGAGCAACTTAC ACCTCC, IL-23 R: GGCAGCTATGGCCAAAAGG; Lymphotoxin β F: ACGGGTCGTTATGGTACACG, Lymphotoxin β R: CCCTCTCTGTAGTCCACCA; BAFF F: TACCGAGGTTTACGCAACACC, BAFF R: TTCGTATA GTCGGCGTGTCG; TLR7 F: CAAAGCACGCAGCT CAAAGG, TLR7 R: GGGAGCCAAGGACATCTTTCT; TLR9 F: TGACCATTGAGCCCAGAACC, TLR9 R: GCAGTTCCTGTCATGAAGA; PAD4 F: GGATGGTT GGGCTTCCACAG, PAD4 R: TCCAATGTGCTTTG CGGAGG; NLRP3 F: ACGAGTCTGGTGACTTTGTAT, NLRP3 R: CTTTCTCGGGCGGGTAATCTT.

For real-time PCR, the samples were heated to 95 °C for 30 s, followed by 40 cycles with denaturation at 95 °C for 5 s, annealing and extension at 60 °C for 34 s, and a final extension at 72 °C for 1 min. The expression levels of the mRNAs were then reported as fold change versus sham brain or vehicle-treated neutrophils.

Primary Neutrophil-Enriched Culture and Stimulation

Primary neutrophil-enriched cultures were prepared from bone marrow of 8- to 10-week-old healthy C57BL/6J male mice using EasySep Mouse Neutrophil Enrichment Kit (Stem Cell, Cat. No. 19762) according to the manufacturer's instructions. For polarization, neutrophils were treated with lipopolysaccharide (LPS, 1 μ g/mL, Sigma) and interferon γ (IFN γ , 20 ng/mL, Peprotech) (in RPMI 1640 + 10% FBS for 3 h [8])

to induce N1 phenotype, or TGF β (10 ng/mL, Peprotech) (in RPMI 1640 + 10% FBS for 3 h [8]) to induce N2 phenotype. For NET induction, neutrophils were treated with phorbol 12-myristate 13-acetate (PMA, 20 nmol/L) in serum-free cultured medium (RPMI 1640) for 3 h. Neutrophils without any stimulation were defined as N0. After stimulation, normal culture medium was reapplied to neutrophils and the CM was collected 24 h later.

Quantification of NETs

Formation of NETs was quantified as in a previous study [16]. Briefly, in *in vitro* experiments, NETs were identified with Sytox Green staining. Sytox Green (Invitrogen, 1:30,000 diluted in HBSS) was applied to neutrophils cultured on coverslips for 15 min and washed with HBSS. In *in vivo* analysis of NET formation, brain slices were collected and stained with rabbit anti-CitH3 (1:500, Abcam). Images were collected with a microscope (Nikon). The recorded images were loaded onto ImageJ (NIH) for further analysis, at which time NETs were manually quantified by two blinded observers. Decondensed nuclei (stained with DAPI), which also positively stained with Sytox Green or CitH3 and displayed a cloud-like morphology, were considered NETs and digitally recorded to prevent multiple counts. The percentages of NETs were calculated as the average of at least four fields, normalized to the total numbers of cells.

Primary Macrophage-Enriched Culture

Primary monocytes were prepared from bone marrow of 8- to 10-week-old healthy C57BL/6J male mice using EasySep Mouse Monocyte Isolation Kit (Stem Cell, Cat. No. 19861) according to the manufacturer's instructions. Macrophages were induced with macrophage colony-stimulating factor (M-CSF) for 7 days (50 ng/mL) in culture medium (RPMI 1640 + 10% FBS). As for phagocytic analysis, macrophages were first labeled with CMTPX (Invitrogen) following the manufacturer's instructions. Neutrophils were first exposed to ultraviolet rays for 2 h and then incubated with macrophages (neutrophils:macrophages = 10: 1) for 1 h. After two washes with PBS, macrophages were fixed and permeabilized and neutrophils were stained with rat anti-Ly6G (1:500, BD Biosciences). Macrophage phagocytic ability was calculated as neutrophils per macrophage.

Primary Cortical Neuronal Cultures and OGD

Primary cortical neuronal cultures were prepared from E16–18 embryos of C57BL/6 mice as previously described [15]. Neuronal ischemia was induced with OGD. Briefly, culture medium (Neural basal + B27 + 2% glutamate) was retreated and was replaced by EBSS (Gibco). Neurons were then

incubated in 95% N₂ + 5% CO₂ for 6 h. After OGD, normal neuron medium was reapplied for reperfusion and the CM was collected 24 h later. To investigate the impact of neutrophil polarity to ischemic neurons, neurons were treated with various phenotypes of neutrophils (neutrophils:neurons = 1:4) or neutrophil CM (neutrophil CM:neuron medium = 1:1) right after OGD for 24 h. Neuronal viability was assessed with NeuN staining.

Scanning Electronic Microscopy

Mice were sacrificed at 2 days after tMCAO. Mice were first perfused with 2.5% glutaraldehyde (Sigma). Brain tissues within the infarct (~1.0mm³) were collected and subjected to SEM.

Statistic Analysis

Results in the current study were presented as mean ± standard error of the mean. The differences in the means among multiple groups were analyzed using one- or two-way analysis of variance (ANOVA). When ANOVA showed significant differences, pairwise comparisons between means were tested by Dunnett tests. The Student's *t* test was used for two-group comparisons. In all analyses, *P* < 0.05 was considered statistically significant. To assess correlation between neutrophils in the peripheral blood and stroke outcomes, linear regression analysis was performed. *P* < 0.05 was considered statistically significant in linear regression and *R*² was recorded.

Results

Early Elevation of Neutrophils in Peripheral Blood Indicates Detrimental Outcomes of Ischemic Stroke

A total of 225 patients with acute ischemic stroke diagnosed within 24 h of symptom onset and 56 age- and gender-matched healthy controls were included in the study. Among them, infection was evident in 58 AIS patients. Patient demographics including comorbidities are summarized in Table S1 and the patient inclusion process is displayed in Fig. S1. Compared with healthy controls, the numbers of neutrophils and NLR in peripheral blood increased soon after stroke onset in patients with or without infection (Fig. 1a), among which 30 patients with infection showed neutrophilic granulocytosis (neutrophil count > 7.5 × 10⁹/L). In AIS patients with infections, both neutrophil counts and NLR showed no significant correlation with NIHSS scores or infarct diameters (data not shown). In AIS patients without infection, NLR, but not neutrophil counts, was positively correlated with higher NIHSS scores (Fig. 1b, *R*² = 0.07, *P* = 0.0006). To analyze the correlation of peripheral neutrophil elevation with infarct sizes, AIS

patients without infection were divided into two groups: infarction ≤ 1.5 and > 1.5 cm. In patients with infarction ≤ 1.5 cm [9–11], the numbers of neutrophil or NLR did not show significant correlation with infarct sizes (Fig. 1c). Nevertheless, in patients with infarction > 1.5 cm [9–11], both neutrophil counts (*R*² = 0.07, *P* = 0.0208) and NLR (*R*² = 0.07, *P* = 0.0447) positively correlated with patients' infarct sizes (Fig. 1d). These results suggest that early increase of neutrophil in peripheral blood is able to predict worse stroke outcome especially in patients with infarction > 1.5 cm. To better exclude the impact of infection to neutrophil fluctuation and testify the correlation between neutrophil elevation and infarct sizes, male C57/BL6 mice were pretreated with gentamycin (0.8 mg) and streptomycin (4 mg) (s.c./daily) for consecutive 3 days before tMCAO. As expected, the frequency of neutrophil and NLR in peripheral blood positively correlated with infarct volumes of mice at 1 day after tMCAO. Therefore, when eliminating the intervention of infection, elevation of neutrophil indicates detrimental stroke outcome at least during the acute phase of AIS in both patients and animals.

Temporal Dynamics of Neutrophil After Ischemic Stroke

Since neutrophil is associated with stroke prognosis, we further assessed the temporal dynamics of neutrophil in bone marrow, peripheral blood, spleen, and stroke lesion. Male C57/BL6 wild-type (WT) mice were subjected to tMCAO. A drop of neutrophil in bone marrow was detected before 12 h after tMCAO. The frequency of neutrophil in bone marrow then recovered to that of sham-operated mice at 1 day and steadily increased until at least 7 days (Fig. 2a). Accordingly, neutrophil percentages in peripheral blood elevated before 1 day after stroke, followed by a gradual decrease to the level of sham-operated mice at 2 days and maintained at low levels until at least 7 days after tMCAO (Fig. 2a). NLR in peripheral blood showed a more sensitive reflection of neutrophil alteration. Blood NLR increased soon after stroke (6 h), peaked at 12 h–1 day then steadily declined to sham level until 5 days after tMCAO (Fig. S2a). Constitution of neutrophils in spleen elevated soon after tMCAO at 6 h, peaked at 12 h and then steadily declined to the level of sham-operated mice at 2 days after ischemic stroke (Fig. 2a).

To check the infiltration time line of neutrophils in stroke lesion, where neutrophil exerts immunomodulatory functions, expression time courses of chemokines that facilitate neutrophil trafficking (namely, CCL5, CXCL1, CXCL2, CXCL3, CXCL5, CXCL7 [5]) were assessed. We found that mRNA expression of neutrophil attracting chemokines (CCL5, CXCL1, CXCL2, CXCL3) increased rapidly after ischemic stroke, peaked at 12 h, and dramatically decreased to sham level at 48 h (Fig. 2b), while the expression alteration of

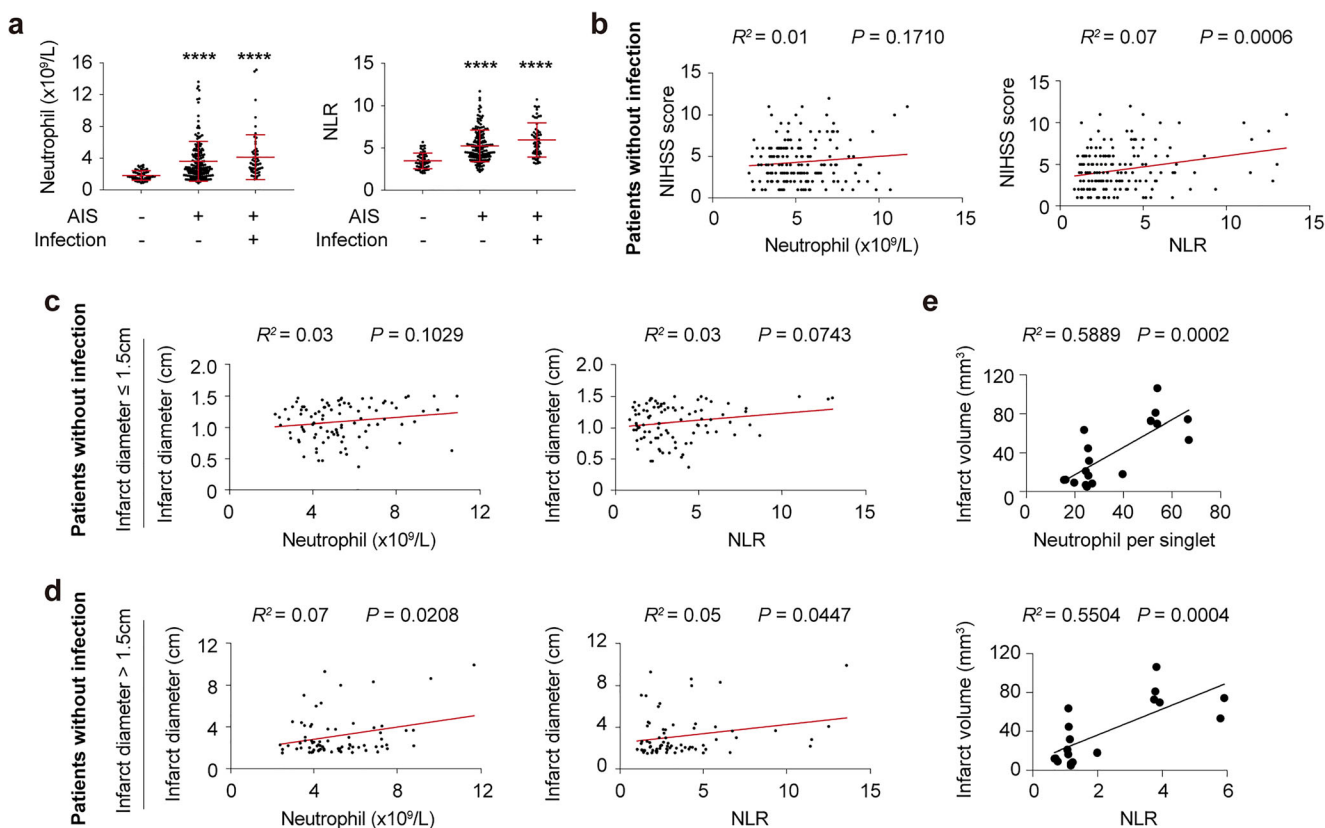


Fig. 1 Early elevation of neutrophil was correlated with detrimental outcomes of cerebral ischemic stroke. A total of 225 patients and 56 age- and gender-matched healthy controls (HC) were included in the study. **a** Comparison of neutrophil count and neutrophil to lymphocyte ratio (NLR) of AIS patients with or without infection and healthy controls (HC). **** $P \leq 0.001$ compared with HC. **b** Linear regression analysis of neutrophil count or NLR with NIHSS scores at admission in AIS patients without infection ($N = 167$). **c, d** Correlation of neutrophil count or NLR

with infarct diameter in patients without infection. Included AIS patients without infection were further divided into small infarction group (infarct diameter ≤ 1.5 cm, $N = 93$) (**c**) and large infarction group (infarct diameter > 1.5 cm, $N = 74$) (**d**), and linear regression analysis of infarct size and neutrophil of the two groups was performed, respectively. **e** Linear regression analysis of neutrophil count or NLR with infarct volume of mice at 1 day after tMCAO ($N = 18$)

CXCL5 and CXCL7 was not detected (data not shown). To identify neutrophil infiltration pattern in stroke lesions, flow cytometry analysis and immunostaining experiments were performed. Notable neutrophil infiltration was first detected at 12 h after tMCAO, right after the expression peak of neutrophil attracting chemokines (12 h). Neutrophil infiltration was prominent at 1–2 days after stroke, when the neutrophil frequency peaked in peripheral blood. Neutrophil cell counts then decreased over time. Before 7 days after tMCAO, few neutrophils were present in the ischemic hemisphere (Fig. 2c). In compliance with flow cytometric analysis, data from immunostaining experiments further confirmed the prominent accumulation of neutrophils in stroke lesion at 1–2 days after cerebral ischemia (Fig. S2b).

Neutrophils regulate poststroke neural inflammation through various inflammatory mediators, including NE, myeloperoxidase (MPO), matrix metalloproteinase (MMP), tissue inhibitor of metalloproteinase (TIMP), interferon (IFN), interleukin (IL), toll-like receptor (TLR), nucleotide-binding oligomerization domain-like receptor (NLR) family

pyrin domain-containing 3 (NLRP3), NET-related peptidylarginine deiminase type 4 (PAD4), B cell-activating factor (BAFF), lymphotoxin, etc. To evaluate the expression dynamics of inflammatory mediators related to neutrophil functions, ischemic hemispheres of male WT mice at different time points after tMCAO were collected and qPCR analysis was performed. We documented that mRNA levels of NE, MPO, MMP3, TIMP1, and IL-12 elevated in ischemic brain at 1 day after stroke. MMP10, NLRP3, and BAFF showed increased mRNA levels at 2 days, while mRNA expression of MMP2, MMP8, MMP9, MMP13, IFN γ , IL-23, TLR7, TLR9, and PAD4 was not increased until 3 days after tMCAO (Fig. 2d and Fig. S2c).

Neutrophil Phenotypes and Clearance Dynamics After Ischemic Stroke

It has been previously demonstrated that polarization toward N2 of neutrophils was beneficial to stroke outcome [6]. Nevertheless, neutrophil phenotypic alteration after ischemic

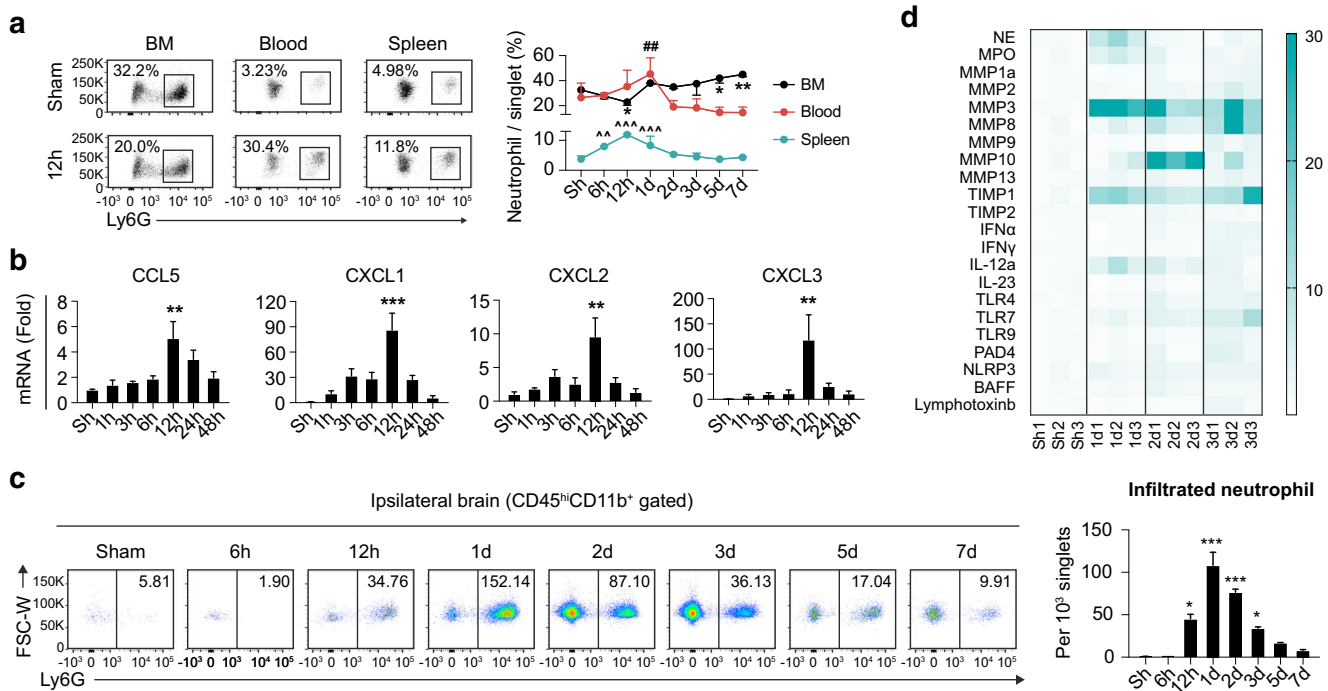


Fig. 2 Temporal and spatial dynamics of neutrophil after ischemic stroke. Male C57/BL6 mice were subjected to 60 min tMCAO and sacrificed at various time points. **a** Neutrophil constitution in bone marrow (BM) blood and spleen of mice as assessed with flow cytometry. $N=3-5$. * $P \leq 0.05$, ** $P \leq 0.01$ versus sham in BM. ### $P \leq 0.01$ versus sham in blood. ^^ $P \leq 0.01$, ^^ $P \leq 0.001$ versus sham in spleen. **b** Expression dynamics of neutrophil attracting chemokines (mRNA level) after ischemic stroke. $N=3$. ** $P \leq 0.01$, *** $P \leq 0.001$ versus sham (Sh). **c** Temporal dynamics of infiltrated neutrophil after ischemic stroke as assessed with flow cytometry. Number in the representative flow panel =

neutrophil per 10³ singlets in ischemic hemisphere. $N=3-5$. * $P \leq 0.05$, *** $P \leq 0.001$ versus sham (Sh). **d** Heat map showing expression dynamics of neutrophil-related inflammatory mediators in the ischemic hemisphere as analyzed with qPCR. $N=3$. Statistics analysis is displayed in Fig. S2c. FSC, forward scatter; W, width; hi, high; NE, neutrophil elastase; MPO, myeloperoxidase; MMP, matrix metalloproteinase; TIMP, tissue inhibitor of metalloproteinase; IFN, interferon; IL, interleukin; TLR, toll-like receptor; NLRP3, nucleotide-binding oligomerization domain-like receptor (NLR) family pyrin domain-containing 3; PAD, peptidylarginine deiminase type; BAFF, B cell-activating factor

stroke has not been documented. In the current study, polarization dynamics of neutrophils was explored with flow cytometry. The macrophage mannose receptor, CD206, has long been regarded as a marker of M2 macrophages and N2 neutrophils [17]. We found that the percentage of CD206⁺ N2 neutrophils in the ischemic brain was relatively stable over time after ischemic stroke, which slightly increased at 7 days after tMCAO (Fig. 3a and Fig. S3a). Constitution of N2 neutrophils in blood and spleen was stable over time (Fig. 3a and Fig. S3a). Overall, mean fluorescence intensity of CD206 on infiltrated neutrophils in the ischemic brain was lower than that in blood and spleen (Fig. 3a). Therefore, immunostaining of CD206 on autoMACS-sorted neutrophils was performed. Although at a relatively low level, expression of CD206 on infiltrated neutrophils in the ischemic brain was confirmed (Fig. S3b).

The protective effect of N2 neutrophils was at least partially dependent on their preferential clearance by microglia/macrophages, thus promoting neural inflammatory resolution [6]. Therefore, neutrophil clearance time courses and the correlation with N2 polarization were explored. Singlets in the ischemic hemisphere were

permeabilized and labeled with antibody cocktail (anti-CD45-PerCP/Cy5.5, anti-CD11b-PE, anti-Ly6G-APC/Cy7, and anti-F4/80-BV421). CD45^{hi}CD11b⁺Ly6G⁺F4/80⁺ cells were determined as neutrophils engulfed by microglia/macrophages, while CD45^{hi}CD11b⁺Ly6G⁺F4/80⁻ cells were recognized as unengulfed neutrophils (Fig. 3b). The process of neutrophil clearance by microglia/macrophages started as early as 12 h and peaked at 2 days after stroke. The phagocytic process continued over time until at least 7 days after tMCAO (Fig. 3c and Fig. S3c). Immunostaining of Iba1 and Ly6G confirmed that Iba1⁺Ly6G⁺ engulfed neutrophils were mostly detected at 2–3 days after tMCAO (Fig. 3d). To explore the impact of neutrophil phenotype on neutrophil clearance, mean fluorescence intensity (MFI) of CD206 on CD45^{hi}CD11b⁺Ly6G⁺F4/80⁺ cells and CD45^{hi}CD11b⁺Ly6G⁺F4/80⁻ cells was compared. Interestingly, CD45^{hi}CD11b⁺Ly6G⁺F4/80⁺ cells showed lower expression of MPO (Fig. 3f and Fig. S3d) but higher MFI of CD206 over time (Fig. 3e and Fig. S3d), although CD206 expression in neutrophil-infiltrated stroke lesions was relatively stable.

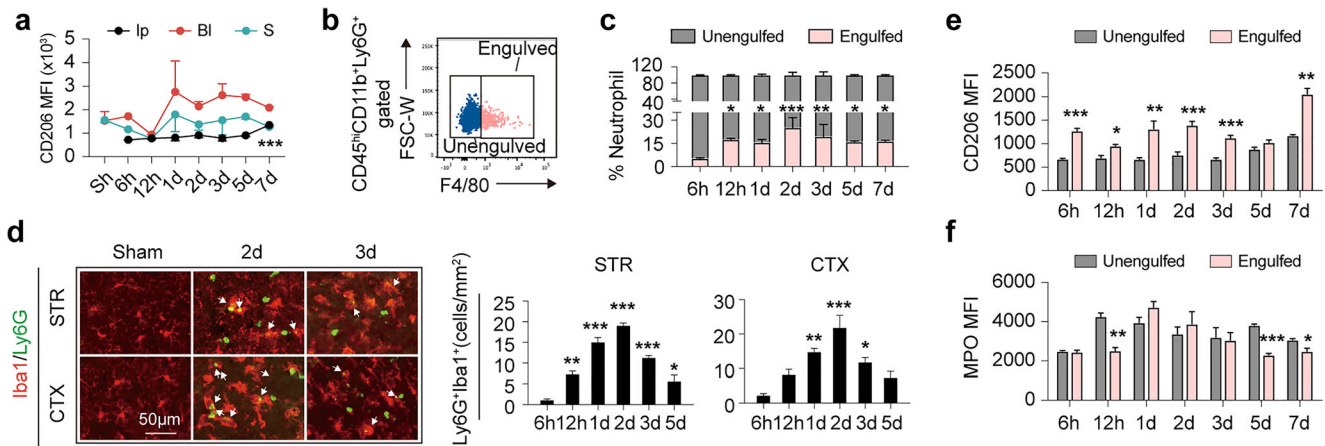


Fig. 3 Polarization and clearance dynamics of neutrophil after ischemic stroke. **a** Polarization dynamics of neutrophils were assessed by CD206 expression with flow cytometry. Mean fluorescent intensity (MFI) of CD206 on neutrophils in ipsilateral brain (Ip), blood (Bl), and spleen (S) was analyzed. $N=3-5$. $***P\leq 0.001$ versus sham in Ip brain. **b** Gating strategy of engulfed neutrophil ($CD45^{hi}CD11b^{+}Ly6G^{+}F4/80^{+}$) and unengulfed neutrophils by macrophage ($CD45^{hi}CD11b^{+}Ly6G^{+}F4/80^{-}$). **c** Flow cytometry analysis of neutrophil clearance by macrophage

at indicated time points. $N=3-5$. **d** Immunostaining of macrophages/microglia ($Iba1^{+}$, red) phagocytosis of neutrophils ($Ly6G^{+}$, green) in stroke lesions at indicated time points. White arrows show neutrophil engulfed by microglia/macrophage. $N=3-4$. **e**, **f** Comparison of CD206 and MPO expression in engulfed and unengulfed neutrophils by macrophages in ipsilateral brain as analyzed with flow cytometry. $N=3-5$. $*P\leq 0.05$. $**P\leq 0.01$, $***P\leq 0.001$, compared with 6 h

Skewing Neutrophil Polarity Toward N2 Phenotype Protected Against Ischemic Stroke

To better address the impact of neutrophil polarity on ischemic stroke, we induced N1 phenotype with $IFN\gamma$ (40 ng/mL) + LPS (1 μ g/mL) and N2 phenotype with $TGF\beta$ (20 ng/mL) in vitro. $IFN\gamma$ + LPS induced N1 neutrophil that showed an elevated mRNA expression of N1 markers $IFN\gamma$ and $TNF\alpha$ (Fig. S4a), while $TGF\beta$ induced N2 neutrophil that had increased mRNA expression of CD206, arginase 1, and IL-10 (Fig. S4b). As assessed with flow cytometry, expression of CD206, the commonly used N2 marker, dramatically increased after $TGF\beta$ treatment (Fig. S4c) as well as the functional cytokine IL-10 production (Fig. S4d). Notably, in neutrophil before (N0) or after $TGF\beta$ treatment (N2), $CD206^{+}$ cells displayed prominently higher expression of IL-10 than $CD206^{-}$ cells (Fig. S4e).

To evaluate the impact of neutrophil polarity on survival of ischemic neuron in vitro, primary mouse neurons were first subjected to 6 h OGD, then were treated with neutrophil CM or co-cultured with different subsets of neutrophils (Fig. 4a). Treatment of N0 or N2 CM failed to cause further decline in neuron counts after OGD, while N1 CM exacerbated post-OGD neuronal death (Fig. 4b). In comparison, neurons co-cultured with N0 or N1 neutrophils were further lost after OGD, while co-culturing with N2 neutrophils hardly affected the viability of ischemic neurons (Fig. 4b). A previous study indicated that N2 neutrophil protected against ischemic stroke at least partially dependent on their promotion of self-clearance by microglia/macrophage [6]. To testify the impact of neutrophil polarity on macrophage phagocytic activities, we subjected neutrophils to macrophage phagocytosis assay.

Indeed, N2 neutrophils facilitated macrophage phagocytosis in vitro, while N1 showed no impact on macrophage engulfment (Fig. S4f).

To further analyze the impact of N2 neutrophil on stroke outcome, $TGF\beta$ was injected to mice at 1 day before tMCAO to skew neutrophil toward N2 phenotype (Fig. 4c). As the proportion of N2 neutrophil increased (Fig. 4d), infarct volumes of mice declined (Fig. 4e), which confirmed that skewing neutrophils toward N2 phenotype was protective to cerebral ischemic stroke.

Time Courses of Neutrophil Extracellular Trap Formation After Ischemic Stroke

Formation of NETs is a process that combats invading microbes. Although the molecular mechanism of NETs remains to be elusive, citrullination of histone [18] and reactive oxygen species (ROS) proceeded by MPO [7] have been proven to be indispensable for NET formation. It is not until recently that NETs were detected in aseptic lesions [8]. In the current study, we documented NETs in ischemic lesions by co-labeling CitH3 and Ly6G (Fig. 5a). We found that NET formation peaked at 2–3 days after ischemic stroke within the stroke lesion in both the striatum and cortex (Fig. 5b). In consistence, NET formation was detected with immunol staining of chromatin dye Sytox Green (green) and NE (red) in stroke lesion with fluorescence microscopy (Fig. 5c) and with SEM (Fig. 5d) at 2 days after tMCAO. Since MPO plays a critical role in NET formation, expression dynamics of MPO in neutrophils was assessed with flow cytometry. In neutrophils infiltrated into the ipsilateral brain, MPO MFI was highest at 1 day after tMCAO, right before the peak of NET formation (Fig. 5d and

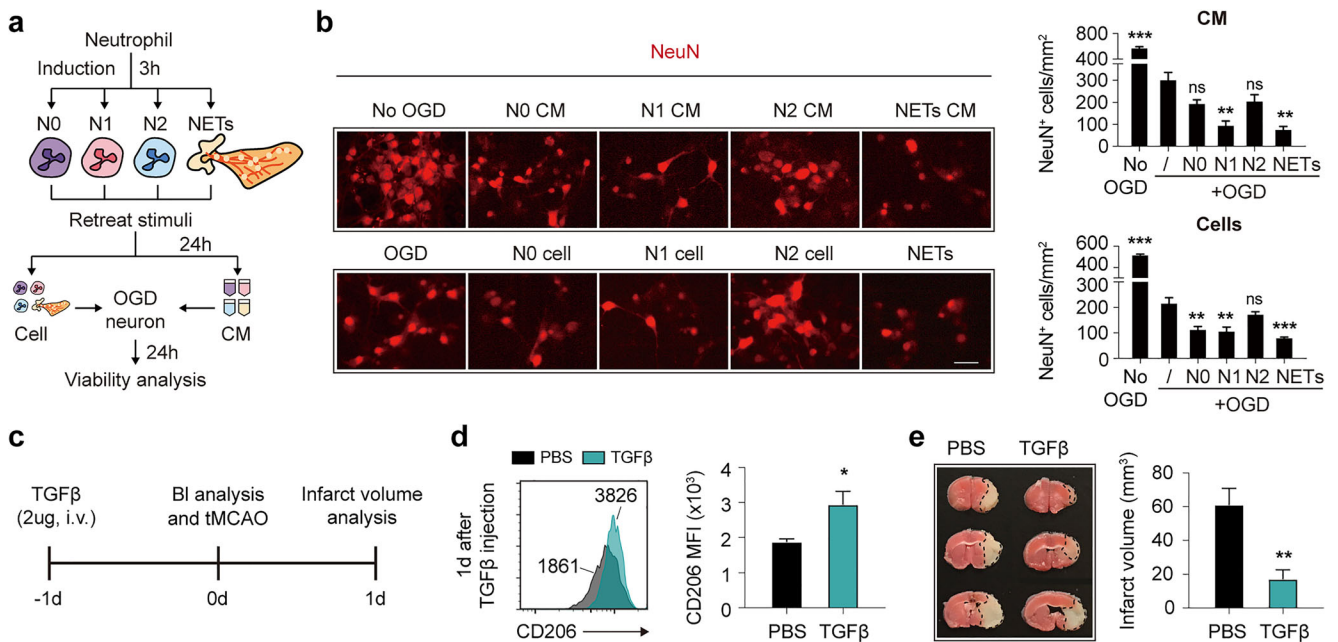


Fig. 4 Protection of N2 neutrophil against ischemic stroke. Neutrophils were isolated from bone marrow of male C57/BL6 mice with magnetic sorting. **a** Time line of neutrophil induction and treatment to ischemic neuron. **b** Viability of ischemic neuron was assessed with immunostaining of anti-NeuN antibodies (red). Data were summarized from three independent experiments. ***P* ≤ 0.01, ****P* ≤ 0.001 versus OGD neuron without treatment. Scale bar = 20 μm. **c** Time line of in vivo N2 induction with TGFβ treatment, tMCAO, and blood (Bl) analysis. **d** Flow

cytometric analysis of neutrophil phenotypic shift at 1 day after TGFβ injection (before tMCAO). *N* = 9 in each group. **P* ≤ 0.05 versus PBS-treated group. **e** Infarct volume analysis at 1 day after tMCAO with TTC staining. Dash line outlined the infarct area. *N* = 9 in each group. ***P* ≤ 0.01 versus PBS-treated group. NETs, neutrophil extracellular traps; OGD, oxygen glucose deprivation; CM, conditioned medium; Bl, blood; TGFβ, transforming growth factor beta; d, day

Fig. S5). In peripheral blood, MPO expression in neutrophils was downregulated at 12 h–1 day after tMCAO and rapidly recovered to the level before stroke (Fig. 5d and Fig. S5).

Surprisingly, MPO MFI of neutrophils in spleen maintained stable over time (Fig. 5d and Fig. S5). The presence of NETs in stroke lesion might exert a detrimental impact on the

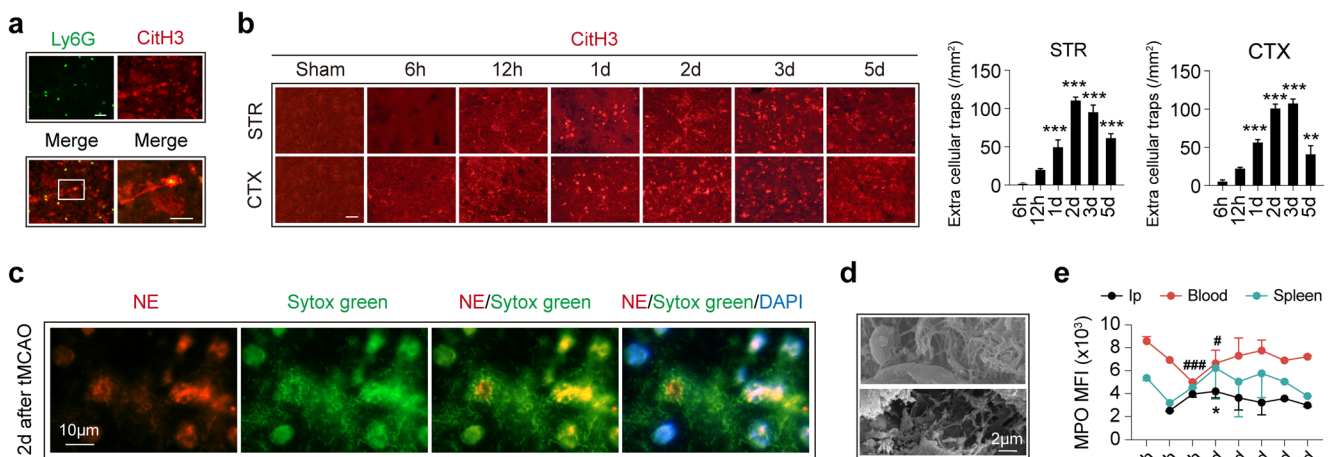


Fig. 5 Neutrophil extracellular trap (NET) formation time course after ischemic stroke. NET formation was analyzed with immunostaining of citrullinated histone 3 (CitH3) in coronal frozen brain slices at different time points after tMCAO. **a** Representative image showing NET formation in striatum stroke lesion (co-localization of Ly6G (green) and CitH3 (red)) at 3 days after ischemic stroke. **b** NET formation dynamics in stroke lesion at the striatum (STR) and cortex (CTX) as assessed with immunostaining of CitH3 (red). NET formation peaked at 2–3 days after tMCAO. *N* = 3–4. ***P* ≤ 0.01, ****P* ≤ 0.001 versus 6 h. Scale bar = 20 μm. **c** Presence of NET formation was confirmed with immunol

staining of chromatin dye Sytox Green (green) and neutrophil elastase (NE) at 2 days after tMCAO. Experiments were repeated for 3 times and representative images from one of the scanning were presented. **d** Presence of NET formation was confirmed with scanning electronic microscopy (SEM) at 2 days after tMCAO. *N* = 4. **e** Expression dynamics of MPO in neutrophil in ipsilateral brain (Ip), blood, and spleen. *N* = 3–4. **P* ≤ 0.05 versus sham in ipsilateral brain; #*P* ≤ 0.05, ###*P* ≤ 0.001 versus sham in blood. CitH3, citrullinated histone 3; STR, striatum; CTX, cortex; d, day; Ip, ipsilateral brain; MFI, mean fluorescence intensity; Sh, sham

already vulnerable neural tissues. In *in vitro* experiments, we found that applying CM of NETs forming neutrophils to ischemic neuron, or co-culturing NETs forming neutrophils with ischemic neuron, could both exacerbate post-OGD neuronal death (Fig. 4b), although NET formation did not affect neutrophil clearance by macrophage (Fig. S4f). Therefore, preventing NET formation could be a promising therapeutic strategy in ischemic stroke.

Neuronal Ischemia Directed Neutrophil Away from N2 Phenotype and Exacerbated NET Formation

Our results showed that N0 CM had almost no impact on neuronal viability, while co-culturing ischemic neurons with N0 cell significantly aggravated neuronal death after OGD, indicating that ischemic neurons manipulated neutrophil functions. To assess the impact of ischemic neurons to neutrophils, OGD conditioned medium (OGD CM) of neurons was used to treat neutrophils (Fig. 6a), and neutrophil polarization and NET formation were assessed. As analyzed with flow cytometry, neuron OGD CM decreased CD206 protein expression in neutrophils (Fig. 6b). Meanwhile, mRNA levels of CD206, Arg1, IL-10, and TGF β were decreased after neuron OGD CM treatment (Fig. 6c). Since NETs had a destructive impact on ischemic neurons and had been detected in the ischemic lesion, we again evaluated whether neuron OGD CM promoted NET formation. As expected, the presence of NETs detected with Sytox Green increased after neuron OGD CM treatment (Fig. 6e) although MPO expression was not affected

(Fig. 6d). In conclusion, ischemic neurons drove neutrophil polarization away from the beneficial N2 phenotype and promoted NET formation.

Discussion

It has been widely recognized that neuroinflammation promotes secondary tissue damage in the ischemic brain [19–24]. Neutrophils are among the first immune cells to infiltrate into brain lesions after ischemic stroke. Timely infiltration of neutrophils is followed by rapid responses within stroke lesions. The present study described and summarized the time course of neutrophil attracting chemokine expression, neutrophil infiltration, neutrophil-related inflammatory alteration, neutrophil polarization, and NET formation. The interaction between neutrophils and macrophages or ischemic neurons was also explored.

Neutrophils in peripheral blood from stroke patients elevated within the first 24 h after symptom onset. Our results suggested that the elevation of neutrophils was positively correlated with stroke outcomes including NIHSS scores and infarct sizes in patients with infarction > 1.5 cm and when infection was excluded, which indicates that early increase of neutrophils in peripheral blood was able to predict worse stroke outcome especially in patients with infarction > 1.5 cm. However, since the NIHSS scores are not sensitive to the lesion sizes, the correlation of neutrophil elevation with NIHSS scores

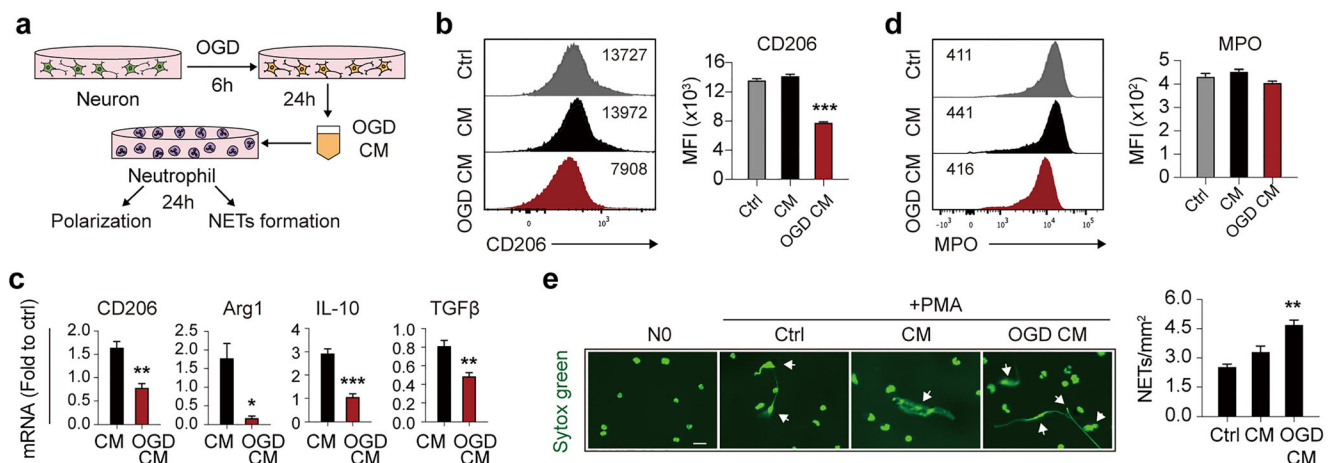


Fig. 6 Impact of neuronal ischemia on neutrophil polarity and NET formation. **a** Time line of neuron conditioned medium after 6 h oxygen glucose deprivation (OGD CM) collection and treatment of neutrophils. **b** Flow cytometric analysis of neutrophil polarity after neuron OGD CM treatment for 24 h with CD206 expression. Data were summarized from three independent experiments. *** $P \leq 0.001$ versus control (Ctrl). **c** Polarization of neutrophils after neuron OGD CM treatment for 24 h was analyzed with mRNA expression of CD206, Arg1, IL-10, or TGF β by qPCR. Data were summarized from three independent experiments. * $P \leq 0.05$, ** $P \leq 0.01$, *** $P \leq 0.001$ versus conditioned medium of

healthy neuron (CM). **d** MPO expression in neutrophils after neuron OGD CM treatment for 24 h was analyzed with flow cytometry. Data were summarized from three independent experiments. **e** Neutrophils were treated with neuron OGD CM for 24 h then subjected to PMA treatment (20 nmol/L for 3 h) to induce NET formation. Neutrophils treated with neuron OGD CM were prone to form NETs. Scale bar = 20 μ m. Data were summarized from three independent experiments. ** $P \leq 0.01$ versus control (Ctrl). OGD, oxygen glucose deprivation; CM, conditioned medium; NETs, neutrophil extracellular traps; h, hour; MFI, mean fluorescence intensity; Ctrl, control; Arg1, arginase 1

and that with infarct sizes was not totally consistent. To better exclude the impact of infections on neutrophil frequency after stroke, mice were pretreated with antibiotics before cerebral ischemia. Correlation of neutrophil counts and infarct sizes was consistent in mice and patients. Since systemic reviews and studies of meta-analysis indicated that preventive antibiotics treatments have little impact on stroke outcome although the incidence of infections might be reduced, we believe that the off-target effects of the antibiotics on stroke outcomes could be neglected. In the current study, part of the included AIS patients had comorbidities, while the interfering factors in mice could be neglected. This explained why the correlation of neutrophil frequency with stroke outcomes in mice was high while that in patients was relatively low. Nevertheless, comorbidities in AIS patients without infection were mostly chronic diseases. Therefore, the comorbidities might not have a great impact on the constitution of neutrophil in patients' peripheral blood. Thus, the data from ischemic stroke models in mice could at least partially reflect the situation in patients.

Increased neutrophil counts in the peripheral blood after the onset of ischemic stroke revealed an acute response by the immune system. From the peripheral blood, neutrophils infiltrate into the stroke lesion and participate in the poststroke neural inflammation. It has documented that neutrophils arrived soon after permanent MCAO and dominant in perivascular areas including leptomeninges (6 h), cortical basal lamina, and cortical Virchow–Robin (15 h) in mice brains as assessed with confocal microscopy [25]. It was not until 24 h that neutrophils were detected in the brain parenchyma [25]. In the current study, we first comprehensively perfused mice with saline then evaluated neutrophil infiltration in the brain parenchyma with flow cytometry. We found that notable neutrophil infiltration was first detected at 12 h and the infiltration into the parenchyma peaked at 1–2 days after transient MCAO, which was in line with the previous study [25].

Infiltrated neutrophils exerted elaborate functions in stroke lesion. Depletion of neutrophils led to decreased infarct volume in stroke mice [6], which altogether indicated that neutrophils played a relative detrimental role in stroke lesions, at least during the acute phase of ischemic stroke. However, neutrophils are the key defense to infection. Thus, decreasing neutrophil population after stroke is not applicable. Since neutrophils exert elaborate functions in the ischemic brain, regulating and controlling neutrophil behavior in stroke lesions could be a therapeutic strategy.

Neutrophils display functional diversity in the ischemic brain. Similar to macrophages, neutrophils show phenotypic plasticity. N1 is the proinflammatory subset for secreting various harmful inflammatory mediators such as

IFN γ and TNF α [26], while the N2 phenotype was shown to be protective in ischemic stroke [6]. In the current study, we found that CD206 expression of neutrophil in stroke lesion had been at a disadvantage until 7 days after tMCAO. In myocardial infarction, which caused aseptic inflammation as in cerebral ischemic stroke, the dynamics of N2 neutrophil showed similar time line with the finding in our experiments. The percentage of CD206⁺ neutrophil increased over time (from $2.4 \pm 0.6\%$ at day 1 to $18.1 \pm 3.0\%$ at day 7) postmyocardial infarction [27]. On the other hand, we found that the macrophage-engulfed neutrophil expressed a significantly higher level of CD206 compared to those unengulfed, which could be a result from stronger phagocytic function of CD206⁺ macrophages or promotion of phagocytosis by CD206⁺ neutrophils. On the other hand, in vitro data confirmed that N2 neutrophils facilitated clearance by macrophages. These results indicate that N2 phenotype promotes self-clearance of neutrophils, which accelerates withdrawal of neutrophils and benefits inflammatory resolution after stroke. Our in vivo data demonstrated that when screwing neutrophil polarization toward N2 phenotype with TGF β pretreatment, stroke outcomes of mice significantly improved. TGF β has efficient anti-inflammatory functions. The effects of reduced disease severity of stroke after TGF β pretreatment may not be solely attributed to increased N2 population. Even so, since TGF β was systemically pretreated and stroke outcomes were evaluated at early time point (1 day) in the study when other immune cells besides neutrophil were still in periphery, the protective effect of systemic TGF β treatment could be largely attributed to N2 polarization of neutrophil. Nevertheless, we argued that solo N2 markers, such as CD206, may not be efficient enough to represent the neuroprotective N2 phenotype. Co-staining neutrophils with multiple N2 markers, including Arg1 and Ym1/2, could be more helpful to distinguish the beneficial cell population.

As for the interaction of neutrophils and neurons, our in vitro data showed that different subsets of neutrophils had differential impact on neuronal viability after OGD. We found that co-culturing neurons with N2 neutrophil cells did no harm to neuronal viability, while N1 or N0 cells exacerbated neuronal death after OGD. Although N2 neutrophils failed to enhance viability of ischemic neurons, the phenotype was less detrimental to the injured neurons. However, neuronal ischemia was prone to drive neutrophils away from the N2 phenotype. Considering the benefit to inflammatory resolution of the N2 population, repolarizing neutrophil toward the N2 phenotype could be a promising therapeutic strategy for ischemic stroke.

Extracellular trap formation is one of the functional characteristics of neutrophils. NET formation was most detected and studied in infectious diseases and was

recently found to be involved in aseptic inflammation [8]. It has been documented that the presence of NETs was a predictor of worse outcomes in myocardial infarction [28] and inhibiting NET formation could efficiently protect against myocardial ischemia [29]. Therefore, formation of NETs might play a detrimental role in aseptic inflammation including ischemic stroke. Nevertheless, understanding of NETs in cerebral ischemia remained to be elusive. The current study showed for the first time that NETs were present in stroke lesions. The function of MPO is indispensable in NET formation [30]. We illustrated that MPO expression in infiltrated neutrophils peaked at 1 day after stroke, before the NETs forming peak were detected (2–3 days), which is in accordance with the processing order of NET formation. Our *in vitro* data demonstrated that neuronal ischemia promoted NET formation, and NETs further increased neuronal death after ischemic injury. Therefore, the adverse impact of NETs to ischemic neuronal tissue is concerning. To inhibit NETs formation or to enhance NETs resolution in stroke lesions could be a therapeutic target for ischemic stroke and both are worthy of in-depth study.

In conclusion, we found that neutrophils are summoned by chemokines and exert elaborated functions in ischemic lesions. Directing neutrophil toward the N2 phenotype protected against ischemic stroke, while N1 and NET formation aggravated the damage of ischemic neurons. Nevertheless, the molecular mechanism of N2 neutrophil interaction with macrophages needs further exploration. NET formation was first identified in stroke lesions in this study. Nevertheless, how NETs were produced and resolved still remains indescribable. Promoting neutrophil polarization toward the N2 phenotype, inhibiting NET formation, or promoting NET resolution could be promising therapeutic targets which reduced neuronal damage after stroke.

Availability of Data and Materials The datasets used and/or analyzed during the current study are available from the corresponding author on reasonable request.

Authors' Contributions W.C. designed and performed the experiments, collected and analyzed data, and drafted the manuscript. S.L. carried out immunostaining, imaging, and quantification and drafted the manuscript. M.H. performed animal experiments and collected data. F.H. and Q.Z. contributed to the experimental design and the manuscript. W.Q. designed the experiment and critically revised the manuscript. X.H. contributed to the experimental design and revised the manuscript. S.G.Z. and Z.L. designed and supervised the study and critically revised the manuscript. J.C. edited and revised the MS. All authors read and approved the final manuscript.

Funding This work was supported by the Chinese Natural Science Foundation (NCSF) grants (81671178 to Z. L.). Z. L. is also supported by the Guangdong Natural Science Foundation grant (2017A030311013).

Compliance with Ethical Standards

Conflict of Interest The authors declare that they have no conflicts of interest.

Ethics Approval All animal experiments were approved by the Third Affiliated Hospital of Sun Yat-sen University and performed following the Guide for the Care and Use of Laboratory Animals and Stroke Treatment. Clinic research was approved by the ethics committee of the Third Affiliated Hospital of Sun Yat-sen University.

Publisher's Note Springer Nature remains neutral with regard to jurisdictional claims in published maps and institutional affiliations.

References

1. Dimagl U, Iadecola C, Moskowitz MA. Pathobiology of ischaemic stroke: an integrated view. *Trends Neurosci.* 1999;22:391–7.
2. Shimamura N, Katagai T, Kakuta K, Matsuda N, Katayama K, Fujiwara N, et al. Rehabilitation and the neural network after stroke. *Transl Stroke Res.* 2017;8:507–14.
3. Gelderblom M, Leyboldt F, Steinbach K, Behrens D, Choe CU, Siler DA, et al. Temporal and spatial dynamics of cerebral immune cell accumulation in stroke. *Stroke.* 2009;40:1849–57.
4. Wu L, Walas S, Leung W, Sykes DB, Wu J, Lo EH, et al. Neuregulin1-beta decreases IL-1beta-induced neutrophil adhesion to human brain microvascular endothelial cells. *Transl Stroke Res.* 2015;6:116–24.
5. Griffith JW, Sokol CL, Luster AD. Chemokines and chemokine receptors: positioning cells for host defense and immunity. *Annu Rev Immunol.* 2014;32:659–702.
6. Cuartero MI, Ballesteros I, Moraga A, Nombela F, Vivancos J, Hamilton JA, et al. N2 neutrophils, novel players in brain inflammation after stroke: modulation by the PPARgamma agonist rosiglitazone. *Stroke.* 2013;44:3498–508.
7. Brinkmann V. Neutrophil extracellular traps in the second decade. *J Innate Immun.* 2018;10:414–421.
8. Lood C, Blanco LP, Pumnalek MM, Carmona-Rivera C, de Ravin SS, Smith CK, et al. Neutrophil extracellular traps enriched in oxidized mitochondrial DNA are interferogenic and contribute to lupus-like disease. *Nat Med.* 2016;22:146–53.
9. Jackson C, Sudlow C. Comparing risks of death and recurrent vascular events between lacunar and non-lacunar infarction. *Brain.* 2005;128:2507–17.
10. Traylor M, Rutten-Jacobs LC, Thijs V, et al. Genetic associations with white matter hyperintensities confer risk of lacunar stroke. *Stroke.* 2016;47:1174–9.
11. Norrving B. Long-term prognosis after lacunar infarction. *Lancet Neurol.* 2003;2:238–45.
12. Lee CF, Venketasubramanian N, Wong KS, Chen CL. Comparison between the original and shortened versions of the National Institutes of Health Stroke Scale in ischemic stroke patients of intermediate severity. *Stroke.* 2016;47:236–9.
13. Sucharew H, Khoury J, Moomaw CJ, Alwell K, Kissela BM, Belagaje S, et al. Profiles of the National Institutes of Health Stroke Scale items as a predictor of patient outcome. *Stroke.* 2013;44:2182–7.
14. Fiebach JB, Stief JD, Ganeshan R, et al. Reliability of two diameters method in determining acute infarct size. Validation as new imaging biomarker. *PLoS One.* 2015;10:e140065.

15. Stetler RA, Cao G, Gao Y, Zhang F, Wang S, Weng Z, et al. Hsp27 protects against ischemic brain injury via attenuation of a novel stress-response cascade upstream of mitochondrial cell death signaling. *J Neurosci*. 2008;28:13038–55.
16. Knight JS, Zhao W, Luo W, Subramanian V, O'Dell AA, Yalavarthi S, et al. Peptidylarginine deiminase inhibition is immunomodulatory and vasculoprotective in murine lupus. *J Clin Invest*. 2013;123:2981–93.
17. Zhang X, Huang F, Li W, Dang JL, Yuan J, Wang J, et al. Human gingiva-derived mesenchymal stem cells modulate monocytes/macrophages and alleviate atherosclerosis. *Front Immunol*. 2018;9:878.
18. Wang Y, Li M, Stadler S, Correll S, Li P, Wang D, et al. Histone hypercitullination mediates chromatin decondensation and neutrophil extracellular trap formation. *J Cell Biol*. 2009;184:205–13.
19. Garcia-Bonilla L, Benakis C, Moore J, Iadecola C, Anrather J. Immune mechanisms in cerebral ischemic tolerance. *Front Neurosci*. 2014;8:44.
20. Zhao H, Garton T, Keep RF, Hua Y, Xi G. Microglia/macrophage polarization after experimental intracerebral hemorrhage. *Transl Stroke Res*. 2015;6:407–9.
21. Wang J, Ye Q, Xu J, Benedek G, Zhang H, Yang Y, et al. DRalpha1-MOG-35-55 reduces permanent ischemic brain injury. *Transl Stroke Res*. 2017;8:284–93.
22. Fan X, Jiang Y, Yu Z, Liu Q, Guo S, Sun X, et al. Annexin A2 plus low-dose tissue plasminogen activator combination attenuates cerebrovascular dysfunction after focal embolic stroke of rats. *Transl Stroke Res*. 2017;8:549–59.
23. Li L, Tao Y, Tang J, Chen Q, Yang Y, Feng Z, et al. A cannabinoid receptor 2 agonist prevents thrombin-induced blood-brain barrier damage via the inhibition of microglial activation and matrix metalloproteinase expression in rats. *Transl Stroke Res*. 2015;6:467–77.
24. Yu IC, Kuo PC, Yen JH, Paraiso HC, Curfman ET, Hong-Goka BC, et al. A combination of three repurposed drugs administered at reperfusion as a promising therapy for postischemic brain injury. *Transl Stroke Res*. 2017;8:560–77.
25. Perez-de-Puig I, Miro-Mur F, Ferrer-Ferrer M, et al. Neutrophil recruitment to the brain in mouse and human ischemic stroke. *Acta Neuropathol*. 2015;129:239–57.
26. Andzinski L, Kasnitz N, Stahnke S, Wu CF, Gereke M, von Köckritz-Blickwede M, et al. Type I IFNs induce anti-tumor polarization of tumor associated neutrophils in mice and human. *Int J Cancer*. 2016;138:1982–93.
27. Ma Y, Yabluchanskiy A, Iyer RP, Cannon PL, Flynn ER, Jung M, et al. Temporal neutrophil polarization following myocardial infarction. *Cardiovasc Res*. 2016;110:51–61.
28. Mangold A, Alias S, Scherz T, Hofbauer T, Jakowitsch J, Panzenböck A, et al. Coronary neutrophil extracellular trap burden and deoxyribonuclease activity in ST-elevation acute coronary syndrome are predictors of ST-segment resolution and infarct size. *Circ Res*. 2015;116:1182–92.
29. Vajen T, Koenen RR, Werner I, Staudt M, Projahn D, Curaj A, et al. Blocking CCL5-CXCL4 heteromerization preserves heart function after myocardial infarction by attenuating leukocyte recruitment and NETosis. *Sci Rep*. 2018;8:10647.
30. Bjornsdottir H, Welin A, Michaelsson E, et al. Neutrophil NET formation is regulated from the inside by myeloperoxidase-processed reactive oxygen species. *Free Radic Biol Med*. 2015;89:1024–35.